On the heat of formation of carbonyl fluoride, CF_2O

Robert L. Asher, Evan H. Appelman, and Branko Ruscic
Chemistry Division, Argonne National Laboratory, Argonne, Illinois 60439-4831

(Received 19 July 1996; accepted 3 September 1996)

In light of the recent controversy surrounding its heat of formation, CF_2O was reexamined by photoionization mass spectrometry. In particular, the CO^+ fragment ion yield curve from CF_2O was interpreted in terms of a retarded $CO^+ + F_2$ process, and a more facile two-step fragmentation to $CO^+ + 2F$. The former process produces a weak, slowly growing tail region without a clear onset, while the latter occurs at higher energy and causes a pronounced growth with a conspicuous onset, which was found to occur at $\leqslant 20.87^{+0.03}/_{-0.07}$ eV at 0 K by fitting with a model curve that incorporates ''fluctuations'' associated with second-generation fragments. This onset leads to $\Delta H^\circ_{f\ 298}(CF_2O) \geqslant -149.1^{+1.4}/_{-0.7}$ kcal/mol, and indicates that the older experimental values for this quantity are too low by at least 3–4 kcal/mol. While the F_2 elimination is retarded by competition with lower energy processes, the two-step process derives its strength from the FCO^+ fragment, which assumes the role of a pseudoparent. Thus, the onset of $CO^+ + 2F$ is expected to appear reasonably close to the thermochemical threshold. Such an interpretation indicates that recently calculated *ab initio* values of -145.3 ± 1.7 kcal/mol and -145.6 ± 1.0 kcal/mol are very likely too high by 3–4 kcal/mol. In addition, the adiabatic ionization potential of CF_2O was refined to 13.024 ± 0.004 eV, while the 0 K appearance potential of the FCO^+ fragment was found by fitting to be $\leqslant 14.752 \pm 0.005$ eV. Together with the suggested value for $\Delta H^\circ_f(CF_2O)$, these two onsets lead to $\Delta H^\circ_{f\ 298}(CF_2O^+) = 151.2^{+1.4}/_{-0.7}$ kcal/mol and $\Delta H^\circ_{f\ 298}(FCO^+) = 173.5^{+1.4}/_{-0.7}$ kcal/mol.
 [S0021-9606(96)00846-X]

I. INTRODUCTION

The apparently well-established JANAF value[1] for the heat of formation of CF_2O, $\Delta H^\circ_{f\ 298}(CF_2O) = -152.7 \pm 0.4$ kcal/mol, (-152.0 ± 0.4 kcal/mol at 0 K) has recently been challenged by *ab initio* calculations, which claim that the tabulated value is too low by at least 6, and perhaps as much as 8 kcal/mol. Using the isodesmic reaction

$$CF_2O + CH_4 \rightarrow CH_2O + CH_2F_2. \tag{1}$$

Montgomery *et al.*[2] obtained $\Delta H^\circ_{f\ 0}(CF_2O) = -143.7$ kcal/mol from G2 theory[3] and -144.8 kcal/mol from CBS-QCI/APNO.[4] With the addition of an error bar of ± 1 kcal/mol, and after correction to 298 K, the latter result becomes their[2] suggested new heat of formation of CF_2O, -145.6 kcal/mol, higher by 7.2 kcal/mol than the JANAF value. Following up on this rather surprising result, Schneider and Wallington[5] performed additional calculations using an approach closely resembling the G2(MP2) method.[6] They reexamined reaction (1) and obtained an even higher value of -143.6 kcal/mol for the heat of formation of CF_2O at 298 K. However, after taking into account the results based on two additional isogyric reaction schemes and the previous results by Montgomery *et al.*,[2] Schneider and Wallington[5] end up selecting $\Delta H^\circ_{f\ 298}(CF_2O) = -145.3 \pm 1.7$ kcal/mol. This is, apart from the error bar, practically identical to the value suggested by Montgomery *et al.*[2]

As further evidence that their inference is correct, Schneider and Wallington[5] show that the introduction of this new higher value for the heat of formation of CF_2O appears to partly reconcile discrepancies between the calculated and experimentally derived heats of formation of CF_3O and CF_3OOCF_3. To reiterate briefly, Bat and Walsh[7] cite a number of experimental results which can be consolidated into $\Delta H^\circ_{r\ 298}(2) = 46.8 \pm 0.5$ kcal/mol and $\Delta H^\circ_{r\ 298}(3) = 21.7 \pm 0.9$ kcal/mol for the following reactions:

$$CF_3OOCF_3 \rightarrow 2CF_3O, \tag{2}$$

$$CF_3O \rightarrow CF_2O + F. \tag{3}$$

Introducing the JANAF value[1] for $\Delta H^\circ_{f\ 298}(CF_2O) = -152.7 \pm 0.4$ kcal/mol leads to $\Delta H^\circ_{f\ 298}(CF_3O) = -155.4 \pm 1.0$ and $\Delta H^\circ_{f\ 298}(CF_3OOCF_3) = -357.6 \pm 1.1$ kcal/mol. The value $\Delta H^\circ_{f\ 298}(CF_3O) = -149.2 \pm 2.0$ kcal/mol recommended on the basis of calculations[8] is about 6 kcal/mol higher than the experimentally derived value. This discrepancy seems to be very similar to that observed for CF_2O. The theoretical ''estimate''[8] for $\Delta H^\circ_{f\ 298}(CF_3OOCF_3) = -342.8 \pm 2.7$ kcal/mol, later quoted[5] as -346.9 kcal/mol, is not really based on an independent calculation. Rather, it is derived by combining one or the other of the calculated values for $\Delta H^\circ_f(CF_3O)$ with the experimental $\Delta H^\circ_r(2)$ given above. It is thus not surprising that it differs from the purely experimental value by roughly twice the discrepancy encountered for CF_2O or CF_3O. However, instead of using the JANAF[1] value for $\Delta H^\circ_{f\ 298}(CF_2O)$, Schneider and Wallington[5] derive pseudoexperimental quantities by combining $\Delta H^\circ_{f\ 298}(2)$ and $\Delta H^\circ_{f\ 298}(3)$ with their suggested theoretical value of -145.3 ± 1.7 kcal/mol, which is 7.4 kcal/mol higher than the JANAF value. With this approach they obtain $\Delta H^\circ_{f\ 298}(CF_3O) = -148.0 \pm 1.9$ kcal/mol and $\Delta H^\circ_{f\ 298}(CF_3OOCF_3) = -342.8 \pm 2.7$ kcal/mol. These values are, of course, higher

than the straightforward experimental values by exactly 7.4 and 14.8 kcal/mol, which brings them into significantly better agreement with theoretical values.

Given the deservedly good reputation of G2 and similar theories, the theoretical inferences by Montgomery *et al.*[2] and by Schneider and Wallington[5] would seem to provide strong evidence that the JANAF[1] value for the heat of formation of CF_2O is indeed too low by 7 to 8 kcal/mol. The tabulated value is essentially based on measurements by von Wartenberg and Riteris,[9] who determined the enthalpy of hydrolysis of CF_2O and reported -26.7 ± 0.2 kcal/mol for the reaction

$$CF_2O(g)+H_2O(l)\rightarrow CO_2(g)+2HF\cdot 300H_2O. \tag{4}$$

When combined with JANAF's own values for $\Delta H^\circ_{f\ 298}(CO_2)=-94.052\pm0.011$ kcal/mol and $\Delta H^\circ_{f\ 298}(HF\cdot 300H_2O)=-76.84$ kcal/mol, this yields the selected $\Delta H^\circ_{f\ 298}(CF_2O)=-152.7\pm0.4$ kcal/mol. As supporting evidence, JANAF also quotes the results by Ruff and Li,[10] who measured the gas-phase equilibrium

$$2CF_2O\rightleftharpoons CO_2+CF_4 \tag{5}$$

in the temperature range 573–1473 K. Subsequently, their data were very carefully analyzed by Stull *et al.*,[11] who excluded the three points at lower temperatures (taken with a nickel catalyst) on the grounds that true equilibrium may not have been reached, and who then used an average of the five higher-temperature points (taken with a Pt catalyst) to derive $\Delta H^\circ_{r\ 298}(5)=-12\pm3$ kcal/mol from a Third Law approach. With JANAF's $\Delta H^\circ_{f\ 298}(CF_4)=-223.0\pm0.3$ kcal/mol, this leads to $\Delta H^\circ_{f\ 298}(CF_2O)=-152.5\pm3.3$ kcal/mol, in excellent agreement with the hydrolysis result, albeit with a larger error bar.

The compilation of Gurvich *et al.*[12] provides a more exhaustive analysis of experimental determinations of $\Delta H^\circ_{f\ 298}(CF_2O)$. These authors present a table with an assortment of reinterpreted values that ''coincide within the uncertainty limits.'' In particular, they obtain -153.0 ± 1.2 kcal/mol from the hydrolysis experiment,[9] and -152.5 ± 1.4 kcal/mol from the Third Law analysis of the five high-temperature points of Ruff and Li.[10] They also list the new equilibrium study by Amphlett *et al.*,[13] which yields -153.7 ± 2.4 kcal/mol by Third Law analysis, a calorimetric measurement by Duus[14] giving -153 kcal/mol, and a Russian measurement[15] by the explosion method in a spherical bomb, reinterpreted to yield -155 ± 2 kcal/mol. For the sake of completeness, Gurvich *et al.*[12] also list the Second Law analysis of the equilibrium measurements, which unfortunately produces only very coarse values of -160 ± 25 and -175 ± 12 kcal/mol. These are, however, ignored in the final analysis, and Gurvich *et al.*[12] settle for an average value of $\Delta H^\circ_{f\ 298}(CF_2O)=-153.0\pm1.2$ kcal/mol, which coincides with their interpretation of the hydrolysis result.

At this point, it seems to be rather clear that the experimental and calculated heats of formation of CF_2O differ by roughly 7 kcal/mol and that the discrepancy is not easily reconciled. Several scenarios are possible:

(a) The experimental determinations of $\Delta H^\circ_f(CF_2O)$ *are wrong*. Each of the experimental determinations considered by the tabulations[1,12] has some weak point. For example, the hydrolysis measurement[9] can be relatively easily criticized on the grounds that the final state is uncertain. The determinations by explosion in a spherical bomb[15] and by calorimetry[14] are subject to a similar, albeit milder criticism. The gas phase equilibrium experiments[10,13] originally contained low-temperature points which had to be excluded from the analysis because equilibrium was not reached within the time frame of the experiment.[11,12] This severely restricts the investigated temperature range, and, together with the scatter in the points, makes Second Law determinations very uncertain.[12] Third Law analysis, on the other hand, puts stricter demands on absolute values of equilibrium constants. Additionally, there have been some questions whether a complete equilibrium has been reached even at the higher temperatures.[12] However, in spite of all the individual criticisms, it does not seem very likely that all measurements are in error by a similar amount. Thus, when taken together, the experimental determinations considered by the tabulations appear to constitute a nontrivial body of evidence suggesting that the correct value for $\Delta H^\circ_{f\ 298}(CF_2O)$ is between -152 and -154 kcal/mol.

(b) The calculated heats of formation are in error and/or their quoted error bars are too small. Although G2 and similar theories have demonstrated a very good track record for small organic compounds, it is not clear at all how accurate they are for fluorine-containing molecules. In fact, until proven otherwise, one can speculate that the calculated heats of formation can deviate significantly, and perhaps even systematically, when several fluorine atoms are present in the same molecule. The fact that the calculated values are higher than the experimental values by similar amounts for both $\Delta H^\circ_f(CF_2O)$ and $\Delta H^\circ_f(CF_3O)$ may be interpreted as an indication of a systematic error. The hypothesis of systematic deviation for compounds rich in fluorine is currently being tested by Curtiss *et al.*[16] The rationale for this supposition lies in the fact that G2 and similar *ab initio* theories are best suited for describing molecules with predominantly covalent bonds. Fluorine, with its extreme electronegativity, hardly fits such a description. However, even if no evidence for systematic deviation is found, one can rather safely state that the error bars quoted by Montgomery *et al.*[2] (±1 kcal/mol) and Schneider and Wallington[5] (±1.7 kcal/mol) are on the optimistic side. Such tight uncertainties have been traditionally quoted for simple organic compounds with two ''heavy'' (i.e., nonhydrogen) atoms. For these types of molecules it has been found empirically that the calculated and experimental values usually agree within 1 kcal/mol. However, this level of accuracy has yet to be demonstrated for highly fluorinated compounds, and a simple transfer of error bars from nonfluorinated compounds seems unwarranted at this point.

(c) The accepted heats of formation for most fluorinated compounds are too low by several kcal/mol. This is really the initial part of argument (b) in reverse and is a nightmare to compilers of thermodynamic tables. In a nutshell, thermody-

namic tables are collections of evaluated cross links between heats of formation of interrelated compounds. In particular, the heats of formation for most fluorinated compounds are pegged to other fluorinated compounds and are thus interdependent. One glimpse of these intricacies has been given earlier in this section, when it became apparent that both $\Delta H_f^\circ(CF_3O)$ and $\Delta H_f^\circ(CF_3OOCF_3)$ depend on $\Delta H_f^\circ(CF_2O)$. One can easily imagine a situation where the relative values of heats of formation are more or less correctly established, but an error in one of the key values propagates throughout the table and causes the absolute values of a whole group of related compounds to be systematically off. However, this source of error can be dismissed in the case of $\Delta H_f^\circ(CF_2O)$. Most experiments considered by the tabulations peg CF_2O either to aqueous HF (hydrolysis) or to CF_4 (gas phase equilibria and the explosion method). Although JANAF[1] uses the superseded[12,17] value for $\Delta H_f^\circ(HF,g)$, the discrepancy (0.18 kcal/mol) is too small to be relevant in this discussion. The suggested JANAF value[1] for $\Delta H_{f\ 298}^\circ(CF_4) = -223.0 \pm 0.3$ kcal/mol is produced by a simultaneous least-squares fit of 23 observations interrelating the heats of formation of seven fluorinated compounds, including $HF(g)$ and $HF(aq)$. However, as JANAF points out, this value is identical to that obtained directly by Greenberg and Hubbard,[18] who performed a very accurate study of the combustion of graphite in fluorine and obtained -223.04 ± 0.18 kcal/mol. The latter value is also selected by Gurvich *et al.*,[12] who list a number of individual experiments that arrive at the same value. Therefore, one can conclude that $\Delta H_f^\circ(CF_4)$ is firmly established, and that it rigidly anchors the thermodynamic scale for other fluorinated compounds.

Thus, of the three scenarios presented, only (a) and/or (b) seem likely. Obviously, additional and independent experimental verifications of $\Delta H_f^\circ(CF_2O)$ are needed at this point. In this paper we try to shed more light on the issue by applying photoionization mass spectrometry techniques, with the aim of finding additional support either for the theoretical ''high'' or experimental ''low'' value for $\Delta H_f^\circ(CF_2O)$.

CF_2O has been recently examined by photoionization by Buckley *et al.*[19] However, these researchers were interested only in the threshold regions of the parent CF_2O^+ and fragment FCO^+ ion, and they did not attempt to determine $\Delta H_f^\circ(CF_2O)$ independently. In fact, Buckley *et al.* use the calculated $\Delta H_f^\circ(CF_2O)$ as a starting point to derive other thermodynamic quantities. In the conclusion of their paper, they cautiously qualify their choice by stating that ''the calculated value for $\Delta H_{f\ 298}^\circ(CF_2O)$ was used because of deficiencies in reported experimental values; however, the 'high,' calculated results clearly needs to be verified by experimental measurement.''

The general approach in obtaining heats of formation by photoionization mass spectrometry is through measurements of fragment appearance potentials (APs). CF_2O is a very small molecule, and it has very few fragments. The two most obvious fragments, FCO^+ and CF_2^+, are not very useful for our purpose, because their heats of formation are either not known independently or are not known accurately enough. Furthermore, as we shall demonstrate, CF_2^+ does not have a thermochemically significant threshold. The CO^+ fragment presents, at least in principle, a possibility, if one could work around the pitfalls usually associated with higher energy fragments. As we shall show in this paper, it is possible to do so in the case of CF_2O, and, propitiously, the approach leads to a reasonable result.

II. EXPERIMENTAL ARRANGEMENT

The photoionization apparatus utilized in this study is a reconstruction of an earlier machine, and it consists essentially of a 3 m vacuum-ultraviolet (VUV) normal-incidence monochromator (McPherson) mated to an experimental chamber which accommodates an ionization region, ion optics, a quadrupole mass spectrometer, and a light detector. The experiments described here utilized the He light source, which generates a smooth Hopfield continuum covering roughly the region between 600 and 1000 Å. The nominal photon resolution was kept at 0.82 Å (FWHM) throughout the experiments. The wavelength scale was accurately calibrated by internal standards consisting of sparse atomic impurity lines belonging to Ne I, N II, and H I and appearing in our light spectrum. The mass-selected ions were pulse counted, while the light intensity was concomitantly recorded by monitoring the fluorescence of a sodium-salicylate-coated window by an external photomultiplier.

Several different samples of carbonyl fluoride were used in these experiments. A commercial product, declared to be of technical purity (85% min.), was obtained from PCR and was found to contain large amounts of CO_2 and CF_4. This sample was used only to produce the overview scans of the parent CF_2O^+ ion and the FCO^+ fragment. Most of the other measurements were performed using homemade samples of CF_2O, which contained no detectable impurities. These samples were synthesized by passing pure CO through a column of AgF_2 attached to a metal vacuum line.[20] The resulting CF_2O product was trapped in a U-tube cooled with liquid nitrogen and transferred to a Monel pressure vessel for storage. These homemade CF_2O samples were introduced into the instrument from an acetone/dry ice bath, which suitably reduced the container pressure and allowed the sample flow to be controlled by a simple in-line needle valve. In order to increase sensitivity and avoid interference from background N_2^+, which appears at the same $m/e = 28$ as $^{12}CO^+$, the final measurements of the CO^+ fragment were performed with $^{13}CF_2O$ samples, which were synthesized from ^{13}CO in the same manner as the samples of normal isotopic composition. The CO, ^{13}CO, and AgF_2 used in the synthesis were of commercial origin (Aldrich).

III. RESULTS

A. Overview and parent ionization

The mass spectrum of CF_2O observed at the He I resonance line (584.33 Å≡21.218 eV) is listed in Table I. Although the relative intensities are somewhat distorted by the inherent mass discrimination function of the quadrupole mass spectrometer, the tabulation provides a good guide to the relative importance of various fragmentation channels. As one can readily see, the FCO^+ fragment is the dominant

TABLE I. Photoionization mass spectrum of CF_2O at 584.3 Å≡21.218 eV. The intensities are not corrected for the quadrupole mass discrimination function. The listed m/e ratios are those corresponding to a sample with natural isotopic composition, although some masses (such as CO^+) were obtained from a $^{13}CF_2O$ sample.

m/e	Species	Relative intensity
66	CF_2O^+	35.2
50	CF_2^+	2.9
47	FCO^+	100.0
31	CF^+	<0.1
28	CO^+	5.2

species at 21 eV, nearly three times more abundant than the parent. The next most intense fragment, CO^+, is about 1/7th the parent intensity, followed by CF_2^+, which is weaker roughly by another factor of 2.

Figure 1 shows an overview of the photoion yield curves of the parent CF_2O^+ and its fragments and covers the region between the ionization threshold at ~950 Å and the shortest explored wavelength, ~580 Å. The relative intensities of the ion yield curves are meaningful, apart from the quadrupole discrimination factors. As one can see, between the ionization threshold and ~740 Å, the parent CF_2O^+ is the dominant ion. In contrast to the analogous CH_2O and CH_2S,[21,22] both of which display an abrupt ionization onset followed by a long plateau, the threshold region of CF_2O is conspicuously rounded, clearly indicating an extended Franck–Condon envelope. Upon further magnification (Fig. 2), one clearly sees a series of rounded steps with superimposed small autoionizing peaks. In the first approximation, the underlying step structure should closely resemble an integral over the vibrational peaks in a photoelectron spectrum. In their acclaimed paper on perfluoro effect in photoelectron spectroscopy, Brundle *et al.*[23] studied, *inter alia*, CF_2O. In their analysis of the high resolution spectrum of the first band, they conclude that the transition ''is very nonvertical and displays a long vibrational progression (at least five members) of 1550 cm^{-1} built upon the origin and upon a single quantum of 530 cm^{-1}.'' They assign the 1550 cm^{-1} progression to ν_1 (C–O stretch), and the 530 cm^{-1} ''possibly'' to ν_3 (F–C–F bend).

Although slightly confused by the presence of small intruding autoionizing peaks (e.g., at 950.0±0.5, 946.9±0.5, 944.8±0.5, 940.5±0.5, 938.4±0.5, 935.6±0.5, 933.7±0.5, 930.8±0.5, 928.7±0.5, 926.8±0.5, 924.7±0.5, 921.8±0.5 Å, etc.), the positions of the midrises of steps in the photoionization spectrum in Fig. 2 correlate very well with the vibrational peaks of the first band in the photoelectron spectrum of Brundle *et al.* Thus the main progression in ν_1 can be observed at 952.0±0.3, 937.8±0.5, 924.5±0.5, 911.7±0.7, and 899±1 Å, which, with a hint of anharmonicity, results in an average spacing for ν_1 of 1540±50 cm^{-1}. The position of the steps of the secondary progression in ν_1, which is displaced from the origin by one quantum of ν_3, are even more confused by the superimposed autoionization. Nominally, they appear to be centered at 947.0±0.5, 932.4±0.5, 918.9 ±0.7, and 906.0±1.2 Å. The structural features of the threshold region reported here agree reasonably well with the

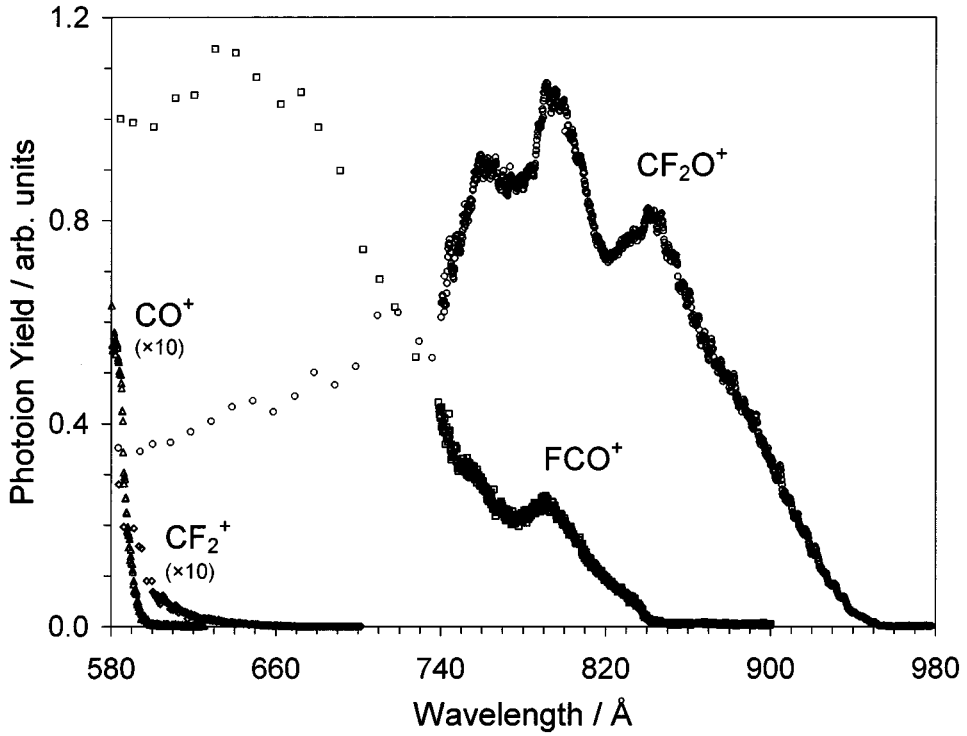

FIG. 1. An overview of the photoion yield curves of CF_2O^+, FCO^+, CF_2^+, and CO^+ between 580 Å and the ionization threshold. The relative abundances of all species are correctly depicted in the figure, apart from quadrupole transmission factors.

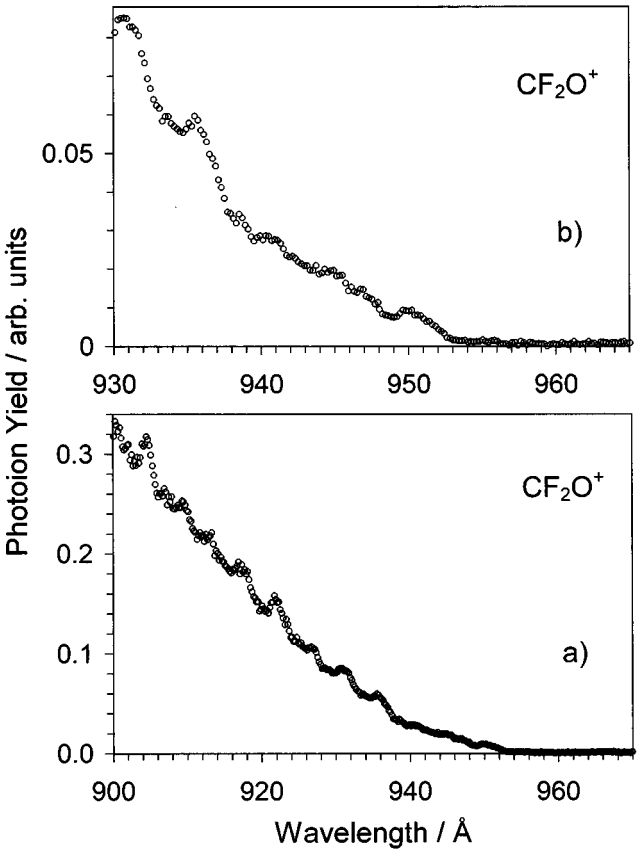

FIG. 2. The expanded threshold region of the CF_2O^+ curve from CF_2O, covering (a) 900 to 970 Å and (b) 930 to 965 Å. The photoion yield curve displays a series of rounded steps with superimposed autoionizing peaks. The underlying step structure reflects the Franck–Condon factors for direct ionization and correlates very well with the vibrational peaks of the first band in the photoelectron spectrum of Ref. 23. The midrise of the first step, at 952.0±0.3 Å≡13.024±0.004 eV, corresponds to the adiabatic IP of CF_2O.

findings of Buckley *et al.*,[19] with the exception that in their case the autoionizing features seem to be curiously less pronounced, in spite of the fact that their reported nominal spectral resolution (0.7 Å) is similar to ours (0.8 Å).

Of particular interest is the midrise of the first step, which occurs at 952.0±0.3 Å≡13.024±0.004 eV and represents the adiabatic IP (ionization potential) of CF_2O. The precise determination of this value has to take into account the fact that there is a small autoionizing peak (at about 950.1 Å) situated close to the top of the underlying step that corresponds to direct ionization. The adiabatic IP derived here is in excellent agreement with the results of Brundle *et al.*,[23] who reported 13.02±0.01 eV, and is in reasonable agreement with the photoelectron study by Thomas and Thompson,[24] who reported 13.04 eV. It is also in apparent agreement with the compilation of Lias *et al.*,[25] who list 13.03 eV without stating the source; their value is presumably the arithmetic average of values reported by Brundle *et al.*[23] and by Thomas and Thompson,[24] rather than an independent determination. Our value is also in good agreement with the previous photoionization study,[19] which reported 13.037±0.020 eV.

Beyond the threshold region, the parent ion yield curve displays prominent autoionizing structure corresponding to several Rydberg states converging to one of the excited electronic states of CF_2O^+. As can be seen in Fig. 1, the structure appears as three broad peaks, with a series of superimposed smaller peaks. The vertical transitions of the two features at lower energy are at about 845–850 and ~800 Å, respectively. The third feature is suggestive of at least two overlapping states, one of lower intensity at ~775 Å, and one of higher intensity at ~765 Å. Essentially, there are only two possible candidates for convergence limits of these Rydberg states: one is the second excited state of CF_2O^+, whose vertical IP was found[23] to be 16.6 eV; the other is the next feature in the photoelectron spectrum,[23] corresponding to a composite of several states, but with an apparently well-defined vertical IP of 17.2 eV. In the photoelectron spectrum, both features have the general shape of a broad peak with partly resolved vibrational substructure near the apex. Although the three features in the CF_2O^+ yield curve are most probably a superposition of various Rydberg states converging to both limits, the interpretation in terms of the 17.2 eV limit is particularly facile. Such a choice would suggest that the first feature is a 3*p* Rydberg, on the grounds of its quantum defect $\delta \approx 0.70$, which is characteristic of an atomic ''*p*'' quantum defect for oxygen (0.710) and/or fluorine (0.752).[26] The second feature is then a 4*s* Rydberg, with $\delta \approx 1.17$, very close to the expected value for an atomic ''*s*'' quantum defect in oxygen (1.142) and/or fluorine (1.201).[26] The vertical transitions of the subsequent members, 4*p* and 5*s*, can be extrapolated by increasing the n^* values by 1, which leads to ~775 and ~760 Å, respectively, and explains the origin of the ''composite'' third feature in the spectrum. There is also a hint of structure at ~753 and ~746 Å, which would correspond to the 5*p* and 6*s* members. This assignment parallels the findings in CH_2O,[21] for which several vibrational members of *ns* and *np* Rydberg states converging to the first and second excited states of the ion were identified and carried quantum defects of ~1.1 and ~0.8, characteristic of oxygen.

B. FCO^+ and CF_2^+ fragments

The first fragment in the photoionization spectrum of CF_2O is FCO^+. A reflection of the autoionizing structure discussed above is clearly discernible in the FCO^+ fragment yield curve. The appearance of autoionizing structure in a fragment yield curve is not an extremely common phenomenon, and it qualitatively signifies that the fragmentation process in question is very competitive. In fact, as the energy increases, the partial cross section shifts so rapidly from the parent to the fragment that FCO^+ becomes the dominant species beyond ~740 Å.

The threshold region of FCO^+, Fig. 3(a), is manifestly non-linear and displays a series of steplike features, which assume a normal peaklike shape at higher energy. The first three features are centered at ~841.3±0.5, ~837.9±0.5, and ~834.2±0.5 Å. They are really autoionization peaks that appear as steps because they are superimposed upon the underlying direct ionization, which exhibits a very sloping be-

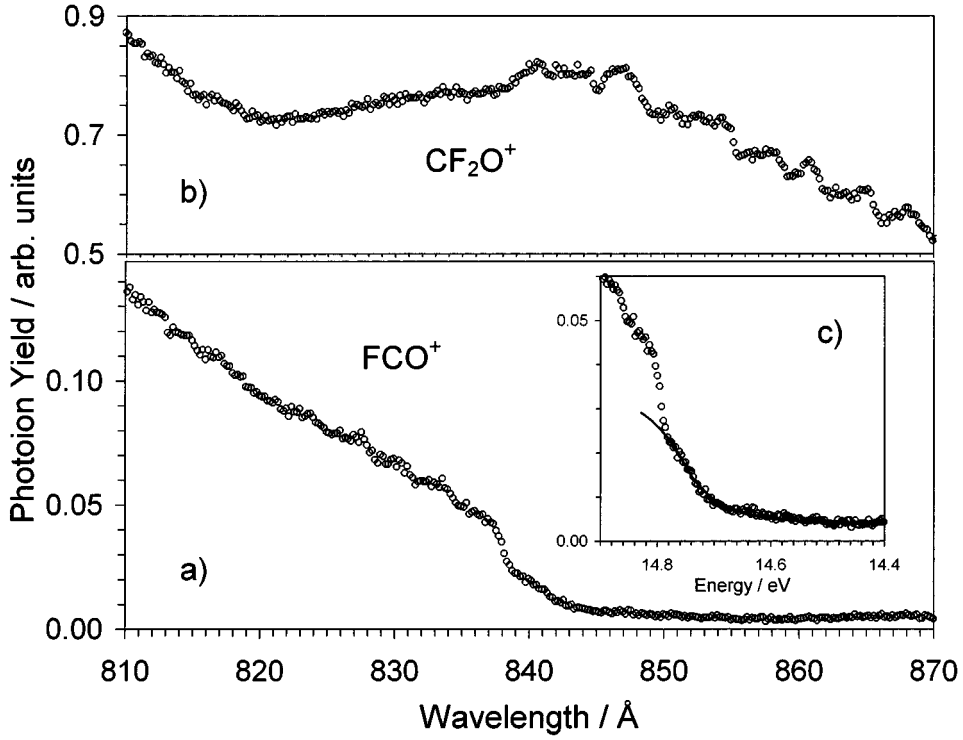

FIG. 3. (a) The threshold region of the FCO^+ curve from CF_2O. The shape of the fragmentation onset is influenced by vibrational autoionization structure, spaced $\sim 500 \pm 50$ cm^{-1}. The structure manifests a steplike shape on the ascending portion of the curve and becomes peaklike at higher energy. (b) The corresponding region of the CF_2O^+ curve from CF_2O shows the same autoionization structure. The vibrational progression seems to shift its intensity from the parent ionization channel to the fragmentation channel. (c) A fit to the lowest-energy steplike feature of the threshold region of the FCO^+ curve from CF_2O. The fit yields $AP_{298}(FCO^+/CF_2O) \leqslant 14.701 \pm 0.005$ eV.

havior near threshold. One should thus not be tempted to correlate these features with the vibrational levels of the first excited state of CF_2O^+, which can be seen in the photoelectron spectrum as a well developed progression of 1450 cm^{-1} (ν_1), with one quantum of ''either 970 or ca. 500 cm^{-1}.''[23] The spacing between these features is $\sim 500 \pm 50$ cm^{-1} and correlates very well with the vibrational structure of the Rydberg state centered at $\sim$845–850 Å in the parent curve [Fig. 3(b)]. In fact, a comparison of Figs. 3(a) and 3(b) suggests that the vibrational progression of the Rydberg state simply shifts its intensity from the parent to the FCO^+ fragment in the neighborhood of the fragmentation threshold.

Figure 3(c) shows a fit to the lowest-energy steplike feature of the threshold region. The general model and the approach are rather similar to those used previously,[27] but the expressions utilized here are slightly more general (see the Appendix). In order to capture the curvature of the first steplike feature, the fit uses a curving kernel of the form $\{1-\exp[-B(h\nu-E_T)]\}$, where $h\nu$ is the photon energy and E_T is the fragmentation threshold. The kernel is convoluted with a function of the form $E^{\eta}\exp(-dE)$, where E is energy, which is a mathematically convenient two-parameter representation of the distribution of the internal energy that is available for fragmentation. The initial form of this broadening function was obtained by fitting the Haarhoff[28] approximate expression for the density of states, which was calculated numerically in the range of interest by using known frequencies for CF_2O.[12,29] During the fits to the experimental data, the kernel position and shape were allowed to change, while the internal energy function was kept fixed in its initial form, as determined by the Haarhoff expression. In a separate set of fits, the shape of the internal energy function was also allowed to change. The initial and the fitted forms of the internal energy function differed only slightly, and produced very similar threshold fits. The AP_{298} threshold values obtained by the two approaches differed only by $\sim$2 meV. Thus the fit of the experimental data does not yield only the inherent appearance potential of FCO^+, but it can also produce an ''experimentally optimized'' internal energy distribution function. The plausibility of the internal energy functions can be checked by calculating the implied average internal energy. Thus the ''experimentally'' derived internal energy function implies $2.11kT$ of available internal energy. For comparison, the normalized Haarhoff function, when numerically integrated, produces $2.15kT$, while standard methods[12,30] yield $1.99kT$ (all at 298 K).

The threshold value derived from the best fit is $AP_{298}(FCO^+/CF_2O) \leqslant 14.701 \pm 0.005$ eV. Buckley *et al.*[19] obtain a higher number (14.736 ± 0.012 eV) for this threshold. However, their value is based on a linear extrapolation of what was rather arbitrarily selected to represent a short quasilinear section near the threshold. In addition, their FCO^+ fragment spectrum suffers from a sharply sloping spurious background, which further confuses their interpretation of the threshold.

Looking back at Fig. 1, one can see that the next frag-

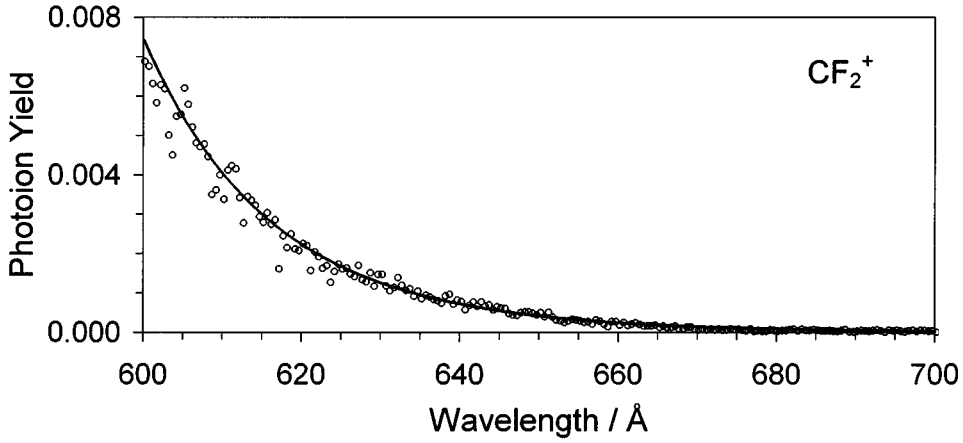

FIG. 4. The CF_2^+ fragment yield curve from CF_2O. The whole curve can be fitted by a simple exponential function, demonstrating that it is impossible to distinguish clearly between the exponential thermal ''tail'' and the onset of this process. The process is heavily retarded by competition from phase space with the FCO^+ fragmentation, which has ~4 eV advantage.

ment (in energy) is CF_2^+, corresponding to the process

$$CF_2O \rightarrow CF_2^+ + O. \tag{6}$$

Compared to formation of FCO^+, the process is very weak and manifests itself as a long and very rounded tail, with no clear onset. It is a classical example of an ill-behaved threshold, suggestive of a process that suffers a significant retardation due to a kinetic shift. That is not very surprising, since (in QET terms) this channel has to compete with the well-developed phase space of the FCO^+ fragmentation process, which is the first fragmentation process and has about 4 eV of advantage. This retards the onset so much that it becomes impossible to distinguish between the post-threshold growth of the fragment ion yield and the pre-threshold exponential thermal tail. In fact, as can be seen in Fig. 4, the whole CF_2^+ fragment ion yield curve can be fitted with a simple exponential function of the form $A\ \exp(\beta E)$. Of course, such an exponential fit has no direct physical meaning. Rather, it clearly demonstrates that this fragment does not produce a thermodynamically relevant threshold.

C. CO^+ fragment

In contrast to the behavior of the CF_2^+ fragment, the CO^+ fragment, which appears at a higher energy, displays a conspicuous and relatively well defined threshold. At first sight, this seems extremely peculiar, since one would expect that the process

$$CF_2O \rightarrow CO^+ + F_2 \tag{7}$$

has to compete not only with the formation of FCO^+ but also with CF_2^+, and thus it should have even more difficulty than CF_2^+ to gain significant cross section. In fact, as we shall see more clearly later, the process responsible for the prominent growth in the CO^+ fragment channel can be associated with the higher energy fragmentation

$$CF_2O \rightarrow CO^+ + 2F \tag{8}$$

which could be viewed as a consecutive process

$$CF_2O \rightarrow FCO^+ + F, \tag{9a}$$

$$FCO^+ \rightarrow CO^+ + F. \tag{9b}$$

This two-step process does not have to compete for phase space with either FCO^+ or CF_2^+. Rather, FCO^+, which is the dominant fragment beyond ~740 Å, acts as a pseudoparent in the second step. Thus compared to the F_2 elimination (and also to the CF_2^+ fragmentation), the $CO^+ + 2F$ channel can be expected to have a much more abrupt and better defined threshold. Another very significant consequence is that the onset of the two-step fragmentation may then be expected to occur reasonably close to the thermochemical threshold.

At this point it is rather instructive to compare the similarities and differences between the fragmentation of CF_2O and the analogous CH_2O. In CF_2O, the $CF_2^+ + O$ asymptote lies about 0.72 eV lower than the $CO^+ + F_2$ asymptote[12] and about 4 eV higher than $FCO^+ + F$. As we have seen in Fig. 4, the 4 eV advantage in phase space of FCO^+ causes a very shallow, exponentially tailing threshold for the $CF_2^+ + O$ channel, which stretches out over several eV and displays no clear onset. The $CO^+ + F_2$ channel, nominally another 0.7 eV higher in energy, will then be suppressed not only by the FCO^+ channel, but also by the fledgling $CF_2^+ + O$ channel, which probably siphons away all the new phase space that becomes available. In the CH_2O case, the $CH_2^+ + O$ asymptote lies 4.2 eV *higher* than the $CO^+ + H_2$ asymptote. Thus the $CO^+ + H_2$ asymptote corresponds to the second rather than to the third fragmentation process and is located only about 1.99 eV above the $HCO^+ + H$ channel. At that point parent ionization is still the dominant process[21] and is roughly two to three times stronger than the HCO^+ fragment. These features translate into significantly less severe phase space competition than in the CF_2O case. In fact, photoionization spectra[21] show a somewhat rounded threshold for $CO^+ + H_2$, apparently retarded by about 0.2 eV (and complicated by the presence of autoionization structure), but showing a relatively reasonable growth past the onset. The two-step $CO^+ + 2H$ channel occurs another 4.4 eV higher in

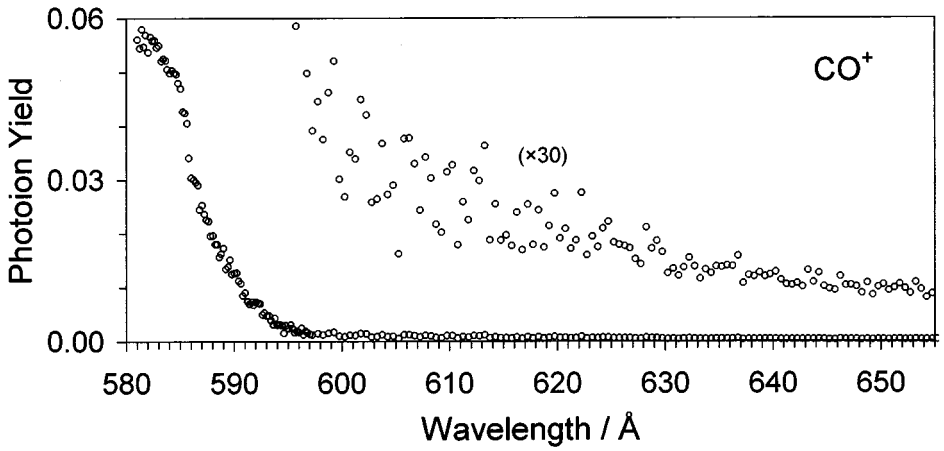

FIG. 5. The $^{13}CO^+$ fragment yield curve from $^{13}CF_2O$. The curve is characterized by two distinct regions, which merge smoothly. The lower energy region displays a very long exponential tail that can be attributed to the $CO^+ + F_2$ fragmentation channel. This channel has to compete for phase space with the $FCO^+ + F$ and $CF_2^+ + O$ channels and is heavily retarded. The higher energy region displays a pronounced growth that can be attributed to the two-step process $CF_2O \rightarrow FCO^+ + F \rightarrow CO^+ + F + F$. This channel does not have to compete for phase space with lower-energy processes. Rather, the FCO^+ fragment, which is dominant in this region, acts as a pseudoparent.

energy. However, at that energy the underlying $CO^+ + H_2$ channel is already fully developed and amounts to almost 10% of the total ion yield. Thus it becomes rather difficult to observe the $CO^+ + 2H$ onset clearly. Nevertheless, a close scrutiny of the fragment ion yield curve of CO^+ from CH_2O does show a moderate increase (of about 10%) at the position appropriate for the $CO^+ + 2H$ process.[21] The relative importance (and thus intensity) of the two processes producing CO^+ depends on a fine interplay of several energy gaps. In the case of CF_2O , the playing field happens to be tilted slightly in favor of the $CO^+ + 2F$ process. Compared to CH_2O, the much larger energy gap between $CO^+ + F_2$ and $FCO^+ + F$ and the intervening $CF_2^+ + O$ asymptote significantly diminish the intensity and retard the appearance of the CO^+ fragment originating from the lower-energy F_2 elimination process. Coupled to this retardation, the smaller gap between the $CO^+ + F_2$ and $CO^+ + 2F$ asymptotes, corresponding to $D_0(F_2) = 1.602$ eV,[31] enhances the relative intensity of the 2F elimination.

Figure 5 shows the fragment photoion yield curve of $^{13}CO^+$ from $^{13}CF_2O$ in greater detail. The photoion yield curve is characterized by two distinct regions that merge rather smoothly. The higher energy region (<590 Å) displays a pronounced growth, while the lower energy region consists of a very long exponential tail, which drags out for about 1.5 eV. The shape of the tail is very reminiscent of the CF_2^+ fragment curve. It has no obvious onset, and it must correspond to the $CO^+ + F_2$ channel.

Figure 6 shows two different fits to the high energy region. The fit in Fig. 6(a) uses a linear kernel convoluted with the internal energy distribution function that was obtained by fitting the FCO^+ fragment. While the fit follows reasonably well the upper portion of the fragment yield curve, it is unable to reproduce the curvature in the tail region. Thus the resulting 298 K appearance potential of 21.01 ± 0.05 eV, which is very similar to the value one would obtain by traditional graphical extrapolation, is only a coarse upper limit to the true value. Substituting the ''experimental'' internal energy distribution function with the one obtained by direct fitting of the Haarhoff expression does not change significantly either the quality of the fit or the threshold value, nor does inserting the curved kernel (as was done for the FCO^+ threshold) instead of the linear one.

The tail region missed by this simple fit has at least two possible contributions. One arises from the underlying F_2 elimination process. Although it is not clear how to exactly apportion intensity to this process, a simple extrapolation of the long exponential tail observed at lower energy suggests that this is a relatively minor contribution. The bulk of the roundness in the tail missed by the fit in Fig. 6(a) can be attributed to ''fluctuations.'' This phenomenon is well known in unimolecular rate modeling of consecutive reactions,[32] and arises from the fact that in a two-step fragmentation process energy can be partitioned in a number of ways between the two first-generation fragments. In mass spectrometry, ''fluctuations'' lead to rounded thresholds that are extremely difficult, if not impossible, to treat correctly by graphical methods, and have been hereto believed to be essentially useless for thermodynamic purposes.[32(c)] However, we have developed a method of properly treating this kind of threshold with our fitting approach. As we show in the Appendix, ''fluctuations'' yield an inherently rounded kernel. Convolution with the internal energy function leads to an analytical expression, which can be readily used for least squares fitting of the experimental data. One of the fitting parameters, β, relates to the ''roundness'' of the threshold, which is in turn associated with the energy gap between the thresholds for the first and second step of the fragmentation.

The result of a fit which includes ''fluctuation'' is shown in Fig. 6(b). The internal energy distribution function used here was the one obtained by fitting the FCO^+ fragment, while the underlying exponential ''background'' associated with the F_2 elimination has been separately determined by fitting the tail region between 650 and 610 Å, and then fixed.

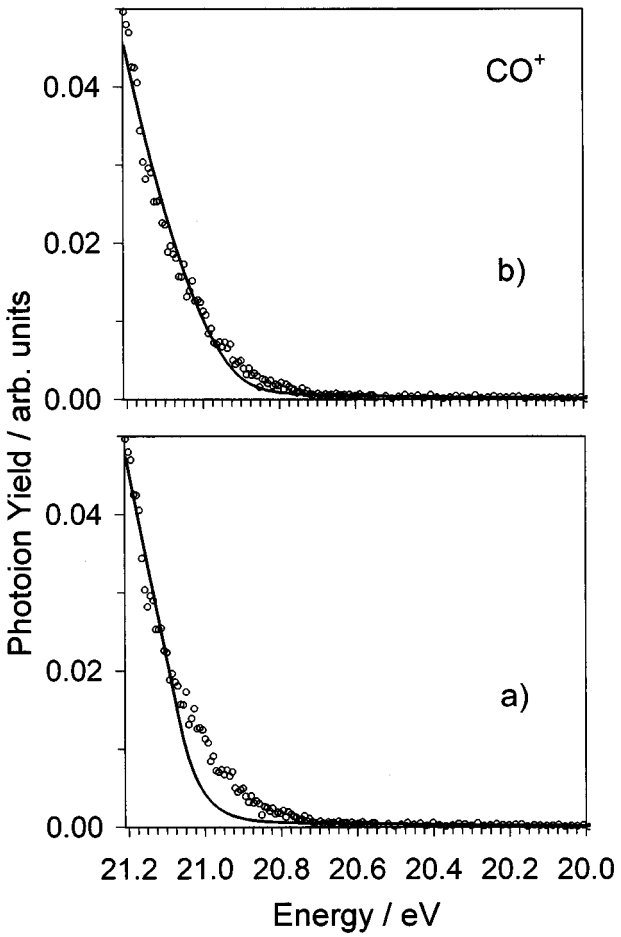

FIG. 6. Two different fits to the high-energy region of the CO^+ fragment. (a) A fit with a linear kernel convoluted by the internal energy distribution function derived by fitting the FCO^+ threshold. This fit underestimates the ''tail'' contributions, because it cannot accommodate the ''fluctuations'' present in a two-step process. The resulting appearance potential, $AP_{298}(CO^+ + 2F/CF_2O) < 21.01 \pm 0.05$ eV, is similar to that which would be obtained by traditional graphical extrapolation methods. The quality of the fit, however, clearly shows that this is just a coarse upper limit. (b) A fit with a curved kernel (see the text) which properly accounts for the effect of the ''fluctuations.'' The resulting appearance potential is significantly lower, $AP_{298}(CO^+ + 2F/CF_2O) \leqslant 20.82^{+0.03}/_{-0.06}$ eV, and likely to be close to the true value.

The resulting 298 K appearance potential is 20.83 eV. As one can immediately see, the fit is substantially better than that in Fig. 6(a). The bulk of the roundness in the tail is correctly reproduced, with only a very small portion of the tail unaccounted for. In an attempt to improve the fit even further, we have tried to vary the components which were held fixed during the fit shown in Fig. 6(b). However, most changes had only a very small impact on the quality of the fit and the resulting appearance potential. One way to obtain a significantly better fit of the experimental data was to ''inflate'' the exponential ''background'' describing the F_2 elimination beyond the point that seems clearly justifiable from the extrapolation of the long wavelength region. While it is quite possible that a simple extrapolation underestimates the relative cross section for this underlying process, the other possibility is that such an ''inflated'' exponential ''background'' has become a mathematical artifact that is trying to absorb the inaccuracies of the fit. Taking into account all these possibilities, we select the 298 K appearance potential for the two-step fragmentation of CF_2O to CO^+ to be $20.82^{+0.03}/_{-0.07}$ eV, where the asymmetric error bar reflects the fact that the fit in Fig. 6(b) slightly underestimates the roundness in the tail. Although technically this is still an upper limit, we believe that this value is relatively close to the true thermochemical threshold for this process, especially in view of the asymmetric error bar quoted.

IV. DISCUSSION

A. Consequences for $\Delta H_f^\circ(CF_2O)$

After correction for the available internal energy of CF_2O[1,12] (0.051_2 eV at 298 K), the strict upper limit to the appearance potential for the $CO^+ + 2F$ channel, $AP_{298}(CO^+ + 2F/CF_2O) < 21.01 \pm 0.05$ eV becomes $AP_0(CO^+ + 2F/CF_2O) < 21.06 \pm 0.05$ eV, and leads to $\Delta H^\circ_{f\ 0}(CF_2O) > -154.2 \pm 1.2$ kcal/mol or $\Delta H^\circ_{f\ 298}(CF_2O) > -153.5 \pm 1.2$ kcal/mol. Although this seems tantalizingly close to the tabulated values, it provides only a coarse lower limit to the heat of formation, and the true value is higher. The more precise appearance potential for CO^+ obtained from the fit that includes the effect of ''fluctuations'', $AP_{298}(CO^+ + 2F/CF_2O) \leqslant 20.82^{+0.03}/_{-0.07}$ eV ($\leqslant 20.87^{+0.03}/_{-0.07}$ eV at 0 K), implies $\Delta H^\circ_{f\ 298}(CF_2O) \geqslant -149.1^{+1.4}/_{-0.7}$ kcal/mol or $\Delta H^\circ_{f\ 0}(CF_2O) \geqslant -148.4^{+1.4}/_{-0.7}$ kcal/mol. This result very strongly suggests that the tabulated 298 K values[1,12] of -152.7 ± 0.4 kcal/mol or -153.0 ± 1.2 kcal/mol are too low, because they fall below our lower limit. On the other hand, the theoretical value recommended by Montgomery *et al.*[2] and by Schneider and Wallington,[5] $\Delta H^\circ_{f\ 298}(CF_2O) = -145.3 \pm 1.7$ kcal/mol, seems slightly too high. It would imply 20.66 ± 0.07 eV for the $CO^+ + 2F$ threshold at 298 K, which is rather far in the tail region of the spectrum and does not seem very likely.

Since appearance potential measurements technically yield only upper limits, the direction of the uncertainty is such that our findings cannot absolutely rule out the calculated value for $\Delta H^\circ_{f\ 298}(CF_2O)$. However, if our interpretation of the origin of the CO^+ fragment ion yield curve is correct, then our upper limit for this appearance potential should be reasonably close to the true value, and $-149.1^{+1.4}/_{-0.7}$ kcal/mol is likely to be the correct value for $\Delta H^\circ_{f\ 0}(CF_2O)$.

Curiously, the value for $\Delta H^\circ_{f\ 298}(CF_2O)$ proposed here is almost exactly midway between the tabulated[1,12] and the calculated[2,5] values (see Table II). Thus, of the original discrepancy of 6–8 kcal/mol between the tabulated and calculated values for $\Delta H^\circ_f(CF_2O)$, about half can be blamed on the tabulated values, which are too low by 3–4 kcal/mol, and half on the calculated values, which appear to be too high by a similar amount.

TABLE II. Ionization potentials, appearance potentials, and heats of formation relevant to present work. The currently recommended values are underlined.

Quantity	This work	Literature values
IP(CF_2O)	$\underline{13.024\pm0.004\ \text{eV}}$	13.02 ± 0.01 eV[a]
		13.04 eV[b]
		13.037 ± 0.020 eV[c]
$AP_0(FCO^+/CF_2O)$	$\underline{\leqslant 14.752\pm0.005\ \text{eV}}$	14.787 ± 0.012 eV[c]
$AP_0(CO^+ + 2F/CF_2O)$	$\underline{\leqslant 20.87^{+0.03}/_{-0.07}\ \text{eV}}$	21.04 ± 0.05 eV[d]
	$\underline{<21.06\pm0.05\ \text{eV}}$	21.03 ± 0.02 eV[e]
		20.72 ± 0.04 eV[f]
		20.70 ± 0.07 eV[g]
IP(FCO)	$9.2_5\pm0.1$ eV[h]	9.30 ± 0.10 eV[c]
		8.76 ± 0.32 eV[i]
$\Delta H^\circ_{f\ 298}(CF_2O)$	$\underline{\geqslant -149.1^{+1.4}/_{-0.7}\ \text{kcal/mol}}$	-153.0 ± 1.2 kcal/mol[j]
	$\underline{>-153.5\pm1.1\ \text{kcal/mol}}$	-152.7 ± 0.4 kcal/mol[k]
		-145.6 ± 1.0 kcal/mol[l]
		-145.3 ± 1.7 kcal/mol[m]
$\Delta H^\circ_{f\ 298}(CF_2O^+)$	$\underline{151.2^{+1.4}/_{-0.7}\ \text{kcal/mol}}$	147 kcal/mol[n]
$\Delta H^\circ_{f\ 298}(FCO^+)$	$\underline{173.5^{+1.4}/_{-0.7}\ \text{kcal/mol}}$	160 kcal/mol[n]
		178.1 ± 2.3 kcal/mol[c]
$\Delta H^\circ_{f\ 298}(FCO)$	...	-43 ± 10 kcal/mol[j]
		-41 ± 15 kcal/mol[k]
		-43.7 ± 2.3 kcal/mol[o]
		-36.4 ± 2.7 kcal/mol[c]
$\Delta H^\circ_{f\ 298}(CF_3O)$	...	$\underline{-151.8^{+1.7}/_{-1.1}\ \text{kcal/mol}}$[p]
		$\underline{-149.2\pm2.0\ \text{kcal/mol}}$[q]

[a]Reference 23.
[b]Reference 24.
[c]Reference 19.
[d]Indirectly, by using $\Delta H^\circ_f(CF_2O)$ from Ref. 12 and other standard thermochemical values from Refs. 1, 12, and 25.
[e]Indirectly, by using $\Delta H^\circ_f(CF_2O)$ from Ref. 1 and other standard thermochemical values from Refs. 1, 12, and 25.
[f]Indirectly, by using $\Delta H^\circ_f(CF_2O)$ from Ref. 2 and other standard thermochemical values from Refs. 1, 12, and 25.
[g]Indirectly, by using $\Delta H^\circ_f(CF_2O)$ from Ref. 5 and other standard thermochemical values from Refs. 1, 12, and 25.
[h]Indirectly, by using our $AP(FCO^+/CF_2O)$, and data from Refs. 35 and 36.
[i]Reference 33.
[j]Reference 12.
[k]Reference 1.
[l]Reference 2.
[m]Reference 5.
[n]Reference 25.
[o]Indirectly, by using data from Refs. 35 and 36.
[p]Indirectly, by using data from Ref. 7 and the currently recommended value for $\Delta H_f(CF_2O)$.
[q]Reference 8.

B. Other consequences

In Sec. III A we have obtained $IP(CF_2O)=13.024\pm0.004$ eV. With our suggested value for $\Delta H^\circ_f(CF_2O)$, this leads to $\Delta H^\circ_{f\ 0}(CF_2O^+)=151.9^{+1.4}/_{-0.7}$ kcal/mol (or $151.2^{+1.4}/_{-0.7}$ kcal/mol at 289 K).

In Sec. III B we have determined $AP_{298}(FCO^+/CF_2O)\leqslant 14.701\pm0.005$ eV, which becomes 14.752 ± 0.005 eV at 0 K and leads to $\Delta H^\circ_{f\ 0}(FCO^+)\leqslant 173.3^{+1.4}/_{-0.7}$ kcal/mol ($173.5^{+1.4}/_{-0.7}$ kcal/mol at 298 K).

If IP(FCO) were accurately known, one could easily derive $\Delta H^\circ_f(FCO)$ and $D_0(F-CFO)$. Unfortunately, that IP is presently not known very well. Dyke *et al.*[33] have examined FCO by photoelectron spectroscopy and concluded that it is extremely difficult to determine the adiabatic IP directly, because the ionization involves a bent-to-linear transition that produces an extremely broad Frank–Condon envelope. This situation is quite parallel to that found for the analogous HCO and HCS radicals.[22,34] After performing a Franck–Condon analysis, Dyke *et al.*[33] bravely concluded that the adiabatic IP was 8.76 ± 0.32 eV, which is 21 vibrational quanta lower than the lowest experimentally observed feature (10.47 ± 0.01 eV). Their error bar reflects an uncertainty

of ± 4 quanta. Buckley *et al.*[19] have recently examined FCO by photoionization and have been able to establish directly only an upper limit of about 9.7 eV. From *ab initio* calculations these authors obtain 9.23 eV, and after attempting to recalibrate the theoretical result by comparisons with known IPs of HCO and CF, they eventually select 9.30 ± 0.10 eV. If the latter is correct, it would mean that the Franck–Condon analysis of Dyke *et al.*[33] is in error by about 7 vibrational quanta, which is perhaps not entirely surprising, given the amount of extrapolation that was necessary in their case. Using our $AP_0(FCO^+/CF_2O)$ and $IP(FCO)=9.3\pm0.1$ eV from Buckley *et al.*[19] gives $D_0(F–CFO)=125.7\pm2.3$ kcal/mol (127.1 ± 2.3 kcal/mol at 298 K), while $IP(FCO)=8.76\pm0.32$ eV from Dyke *et al.*[19] yields $D_0(F–CFO)=138.2\pm7.4$ kcal/mol (139.6 ± 7.4 kcal/mol at 289 K). The former value for the C–F bond energy in CF_2O seems to be more in line with conventional chemical wisdom. For example, the JANAF value[1] for $\Delta H^\circ_{f\ 298}(FCO)=-41\pm15$ kcal/mol is essentially derived by taking $D_{298}(F–CFO)\approx128\pm15$ kcal/mol, which comes from partitioning the two successive C–F bond energies in CF_2O in a 4:1 ratio. Gurvich *et al.*[12] select $\Delta H^\circ_{f\ 0}(FCO)=-43\pm10$ kcal/mol, relying primarily on the work by MacNeil and Thynne,[35] who determined the onset of the dissociative electron attachment process

$$CF_2O+e^-\rightarrow FCO+F^- \tag{10}$$

to be 2.1 ± 0.1 eV at 0 K. When combined with the well-known[36] electron affinity $EA(F)=3.401\ 190\pm0.000\ 004$ eV, this yields $D_0(F–CFO)=126.9\pm2.3$ kcal/mol (128.2 ± 2.3 kcal/mol at 298 K). Combining this value of D_0 with our $AP_0(FCO^+/CF_2O)=14.752\pm0.005$ eV yields $IP(FCO)=9.2_5\pm0.1$ eV, close to the value calculated by Buckley *et al.*,[19] although perhaps one vibrational quantum lower. This IP obviously need further experimental verification.

Finally, use of the suggested value for $\Delta H^\circ_f(CF_2O)$, along with $\Delta H^\circ_{r\ 298}(3)=21.7\pm0.9$ kcal/mol inferred from Batt and Walsh,[7] leads to $\Delta H^\circ_{f\ 298}(CF_3O)=-151.8^{+1.7}/_{-1.1}$ kcal/mol, almost 5 kcal/mol higher than their original value[7,37] of -156.7 kcal/mol, but still 2.6 kcal/mol lower than -149.2 ± 2.0 kcal/mol, which was recommended[8] on the basis of theoretical results. It is interesting to note that the theoretically determined values[5,8] for $\Delta H^\circ_{f\ 298}(CF_2O)=-145.3\pm1.7$ kcal/mol and $\Delta H^\circ_{f\ 298}(CF_3O)=-149.2\pm2.0$ kcal/mol produce $\Delta H^\circ_{f\ 298}(3)=22.9\pm2.6$ kcal/mol, in very good agreement with the experimentally deduced[7] 21.7 ± 0.9 kcal/mol. Thus experiment and theory seem to agree rather well on the relative relationship of $\Delta H^\circ_f(CF_2O)$ and $\Delta H^\circ_f(CF_3O)$; it is the absolute scale that differs by several kcal/mol. Schneider and Wallington[5,8] suggested that the culprit are the older experimental values of $\Delta H^\circ_f(CF_2O)$, which are too low by ~7 kcal/mol. Our findings indicate that the tabulated heat of formation of CF_2O is indeed too low, but probably only by about 3–4 kcal/mol, while the balance of the discrepancy in all likelihood originates in the calculation.

V. CONCLUSION

The present photoionization measurements produce a lower limit to the heat of formation of carbonyl fluoride, $\Delta H^\circ_{f\ 298}(CF_2O)\geqslant-149.1^{+1.4}/_{-0.7}$ kcal/mol, which is midway between the older experimental values[1,12] of $\Delta H^\circ_{f\ 298}(CF_2O)=-152.7\pm0.4$ or -153.0 ± 1.2 kcal/mol, and the recently proposed theoretical value[2,5] of $\Delta H^\circ_{f\ 298}(CF_2O)=-145.3\pm1.7$ kcal/mol. Based on our interpretation and fitting of the CO^+ fragment ion yield curve from CF_2O, we conclude that the tabulated values[1,12] are indeed too low by about 3–4 kcal/mol. Although the nature of our measurements is such that the recently proposed calculated value[2,5] cannot be ruled out with absolute certainty, it does appear that these are too high by 3–4 kcal/mol. Obviously, additional experimental determinations and calculations of this quantity are needed in order to tighten the error bar and perhaps fine tune the value. It would be, for example, very interesting to repeat the original gas phase equilibrium and/or calorimetric measurements which led to the tabulated[1,12] low value for the heat of formation of CF_2O, and see if they can be brought into conformity with our suggested value for $\Delta H^\circ_f(CF_2O)$. On the theoretical front, it appears rather pressing to probe how much truth there is in the suggestion that *ab initio* calculations can run into problems when trying to reproduce the heats of formation of heavily fluorinated compounds. Conducting a thorough and conclusive investigation of this kind is a nontrivial task, since, as it now begins to appear, the number of well established experimental heats of formation for this class of compounds may be quite limited.

Note added in proof. Reference 16 has now taken the shape of a formal publication [L. A. Curtiss, K. Raghavachari, C. P. Redfern, and J. A. Pople, J. Chem. Phys. (in press)]. Using the genuine G2 procedure, Curtiss *et al.* obtain $\triangle H^\circ_{f\ 298}(CF_2O)=-148.6$ kcal/mol, in excellent agreement with our current result, but ~3 kcal/mol lower than previous *ab initio* values, which utilized isogyric and/or isodesmic schemes.[2,5] Curtiss *et al.* also find that, in general, the largest deviations between experiment and G2 theory tend to occur for compounds with multiple fluorine atoms.

ACKNOWLEDGMENTS

One of us (B.R.) would like to thank Dr. Joseph Berkowitz for careful reading of the manuscript and subsequent helpful comments. This work was supported by the U.S. Department of Energy, Office of Basic Energy Sciences, under Contract No. W-31-109-ENG-38.

APPENDIX

Traditionally, the appearance potentials for fragmentation processes have been extracted from the ion yield curves by performing a linear extrapolation. Essentially, one tries to locate a linear or quasilinear region of ascent in the immediate vicinity of the threshold, and extrapolate it to the background level. The intersection of the extrapolated line with the background level then becomes the fragment appearance

potential at the temperature of the experiment, and it gets subsequently corrected to 0 K by taking into account the initial internal energy of the parent that is available for fragmentation. If the fragment yield curve displays a conspicuous linear section near the threshold, it is very easy to distinguish between the fragmentation onset and the exponentially shaped tail region that occurs below the threshold and arises from thermally excited molecules. Thus, in straightforward cases, the traditional method gives satisfactory and reliable results. However, very often the linear section is relatively brief (or even nonexistent), and the selection of a threshold relies to a high degree on subjective judgment, which can be influenced by a number of factors, such as experience, instrumental sensitivity, the aspect ratio of the spectrum, the magnification of the threshold region, etc. In these cases it matters very little whether the extrapolation is performed graphically or by a least-squares fit of a straight line. Furthermore, the extrapolation method inherently rejects the information that is contained in the tail region.

Recently,[27] we have begun using a fitting procedure that has a substantially higher degree of objectivity. Basically, this approach produces appearance potentials by a least-squares fit of the threshold region with a model function. As outlined below, the model function is obtained by convoluting a kernel function (the idealized 0 K fragment yield) with the internal energy distribution function. Previously,[27] we have shown the analytical forms of selected model functions, such as those applicable to systems that are adequately described by 4-rotor internal energy distribution function. Here, we try to explicitly give the analytical form of model functions that use a more general internal energy distribution function.

1. The approximate form of the internal energy distribution function

Generally, if the density of states $\rho(E)$ is known, then the internal energy distribution function $P(E)$ is given as

$$P(E)=N_P\rho(E)\exp(-E/kT),$$

where E is the (internal) energy, N_P is the normalization constant, k is the Boltzmann constant, and T is the temperature. An approximate expression for $\rho(E)$ that is reasonably flexible and still convenient for subsequently convolution can be presented in generic form as

$$\rho(E)\propto E^{\eta}\exp(-dE).$$

This leads to

$$P(E)=N_P E^{\eta}\exp(-aE),$$

where

$$a=d+1/kT,$$

$$N_P=a^{\eta+1}/\Gamma(\eta+1)$$

and $\Gamma(r)$ is the gamma function of r,

$$\Gamma(r)=\int_0^{\infty} e^{-t}t^{r-1}\,dt.$$

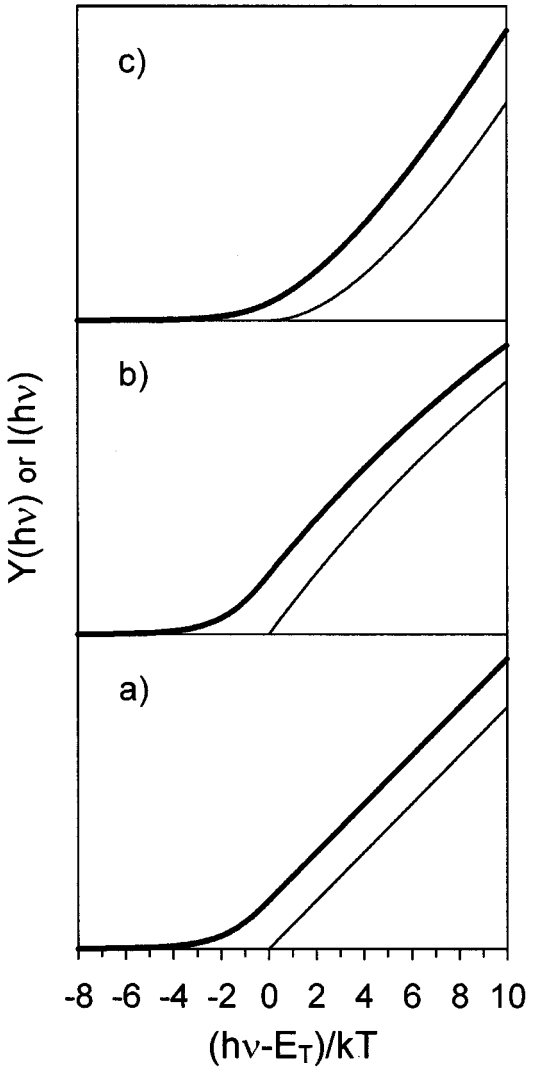

FIG. 7. Examples of three different kinds of kernels, $Y(h\nu)$, and their convolutions, $I(h\nu)$. The kernel (thin line) is the idealized shape of the fragmentation ion yield curve at 0 K. The convoluted form (thick line) takes into account the effect of the internal thermal energy of the parent, $\langle E\rangle$, which is available for fragmentation. For the purpose of illustration, $\langle E\rangle=2\,kT$. The kernel $Y(h\nu)$ intersects the baseline at the thermodynamical threshold E_T. $I(h\nu)$ is shifted toward lower energy by $\langle E\rangle$, and has a rounded, slowly decaying tail region. (a) Linear kernel, $Y_1(h\nu)$ and its convoluted form $I_1(h\nu)$. (b) Exponentially curving kernel $Y_e(h\nu)$ and its convoluted form $I_e(h\nu)$. This kernel accommodates rather easily the frequently observed tendency of the fragment yield curve to level off at higher energy, while maintaining an essentially linear behavior near the threshold. (c) Rounded kernel $Y_f(h\nu)$ and its convoluted form $I_f(h\nu)$. This kernel incorporates ''fluctuations,'' which are present in the threshold region of second-generation fragments. For the purpose of illustration, the parameter β, which defines the extent of ''roundness'' of the kernel, has been chosen such that $1/\beta = 6kT$. The most prominent feature of this kernel is its quadratic behavior near threshold. The convolution adds even more curvature in the threshold region.

The average internal energy associated with $P(E)$ is then

$$\langle E\rangle=\alpha(\eta+1)kT,$$

where

$$\alpha=1/(akT).$$

Note that for $\alpha=1$ (i.e., $d=0$), and $\eta=0, \frac{1}{2}, 1, \frac{3}{2}, \ldots, P(E)$ becomes a correct representation of the internal energy distribution of a q-dimensional rotor, where $\eta = q/2 - 1$. The best initial values for the continuously adjustable parameters η and a (or α) in $P(E)$ can be found by fitting an independently calculated internal energy distribution function based on a density of state function that is believed to represent reasonably well the molecule under scrutiny. Although there are various ways of deriving or calculating the density of states, we have found very useful the expression for $\rho(E)$ given by Haarhoff.[28]

2. The approximate form of the kernel function

The kernel function $Y(h\nu)$ is the inherent shape of the fragmentation threshold at 0 K as a function of photon energy $h\nu$. This function is nonzero only above the threshold, i.e.,

$$Y(h\nu)=0, \quad h\nu<E_T,$$

$$Y(h\nu)\geqslant 0, \quad h\nu\geqslant E_T,$$

where E_T is the 0 K fragmentation threshold. The core shape of the kernel function relates to the integral over the energy deposition function, which in turn depends on the internal states of the parent ion in the region of interest. This shape is further modified by the energy-dependent relationship of the fragmentation rate to the rates of other possible processes. Therefore, kernel functions can display very complicated behaviors, and there is no fundamental reason to expect a linear behavior of the fragmentation threshold, in spite of occasional claims to the contrary. However, it has been found in practice that the fragment yield curve often displays a linear or quasilinear behavior in the vicinity of the threshold region, which is really equivalent to saying that in those cases the energy deposition function is not changing too rapidly in the local region of interest.

So far, we have found empirically[27] two forms of the kernel function that have proven useful in threshold fitting

$$Y_1(h\nu)=A_1(h\nu-E_T)$$

and

$$Y_e(h\nu)=A_e\{1-\exp[-B(h\nu-E_T)]\},$$

where A and B are adjustable parameters [see also Figs. 7(a) and 7(b)]. Of course, $Y_e(h\nu)$ is more flexible because of the additional ''curvature'' parameter B. Past experience suggests [27] that this form of the kernel can accommodate rather easily the frequently observed tendency of the fragment yield curve to level off at higher energy, while maintaining an essentially linear behavior in the immediate vicinity of the threshold. The latter point can be easily demonstrated by series expansion of the exponential function, which yields

$$Y_e(h\nu)\approx A_e\{[B(h\nu-E_T)]-[B(h\nu-E_T)]^2/2!+[B(h\nu-E_T)]^3/3!-\ldots\}.$$

Clearly, the leading term, which is linear, will tend to dominate when $h\nu$ is sufficiently close to E_T and/or when B is small.

3. Convolution of the kernel function with the internal energy function

If $Y(h\nu)$ is the kernel function, and $P(E)$ is the internal energy distribution function, then the experimental fragment ion yield curve recorded at a temperature T can be modeled by $I(h\nu)$, which can be obtained from the following convolution integral:

$$I(h\nu)=\int_{\epsilon_0}^{\infty} Y(\epsilon)P(\epsilon-h\nu)d\epsilon,$$

where $\epsilon_0 = E_T$ if $h\nu < E_T$ and $\epsilon_0 = h\nu$ if $h\nu > E_T$. The solutions to this integral are given below.

(1.1) Linear kernel $Y_1(h\nu) = A_1(h\nu - E_T)$, pre-threshold region $h\nu < E_T$

$$I_1(h\nu)=N_1\{[a(E_T-h\nu)]^{\eta+1}\exp[-a(E_T-h\nu)]+[a(h\nu-E_T)+\eta+1]\Gamma[\eta+1,a(E_T-h\nu)]\}/\Gamma(\eta+1),$$

where $N_1 = A_1/a$, and $\Gamma(r,s)$ is the incomplete gamma function of r,

$$\Gamma(r,s)=\int_s^{\infty} e^{-t}t^{r-1}\,dt.$$

(1.2) Linear kernel $Y_1(h\nu) = A_1(h\nu - E_T)$, post-threshold region $h\nu > E_T$

$$I_1(h\nu)=N_1[a(h\nu-E_T)+\eta+1],$$

where $N_1 = A_1/a$, as in (1.1).

(2.1) Exponential kernel $Y_e(h\nu) = A_e\{1 - \exp[-B(h\nu - E_T)]\}$, pre-threshold region $h\nu < E_T$

$$I_e(h\nu)=N_e\{\Gamma[\eta+1,a(E_T-h\nu)]-\exp[-ba(h\nu-E_T)]\Gamma[\eta+1,a(1+b)(E_T-h\nu)]/(1+b)^{\eta+1}\},$$

where $N_e = A_e/\Gamma(\eta+1)$, and $b = B/a$.

(2.2) Exponential kernel $Y_e(h\nu) = A_e\{1 - \exp[-B(h\nu - E_T)]\}$, post-threshold region $h\nu > E_T$

$$I_e(h\nu)=N_e\{\Gamma(\eta+1)-\exp[-ba(h\nu-E_T)]\Gamma(\eta+1)/(1+b)^{\eta+1}\},$$

where $N_e = A_e/\Gamma(\eta+1)$, and $b = B/a$, as in (2.1).

Both kernels and their convolutions with $P(E)$ are depicted graphically in Figs. 7(a) and 7(b). As one can readily see, the main effect of the convolution is a shift toward lower energies by $\langle E\rangle$ and the appearance of a rounded, slowly decaying tail region.

4. Treatment of fluctuations in consecutive fragmentation processes

When a two-step fragmentation is considered, then the ''fluctuation'' (i.e., partition) of energy among the fragments of the first step has to be taken into account.[32] The probability $\Phi(h\nu)$ that the ionic fragment of the first generation will have internal energy $E \geqslant E_{T2}$ can be given[32(b)] as

$$\Phi(h\nu)=\frac{\int_{E_{T2}}^{h\nu-E_{T1}}\rho_a(\epsilon)\rho_b(h\nu-E_{T1}-\epsilon)d\epsilon}{\int_{0}^{h\nu-E_{T1}}\rho_a(\epsilon)\rho_b(h\nu-E_{T1}-\epsilon)d\epsilon},$$

where E_{T1} and E_{T2} are the threshold energies for the first and the second step, respectively, while $\rho_a(\epsilon)$ and $\rho_b(\epsilon)$ are the densities of states of the two first-generation fragments. The underlying assumption is that the fragmentation rate at energies even only slightly above threshold is sufficiently high when compared to the ion flight time in the mass spectrometer. Although it is clear that contorted transition states will result in a more complicated behavior, the original assumption seems to be valid in most cases.[32] Furthermore, if the neutral counter-fragment in the first step is an atom, then $\Phi(h\nu)$ simplifies into

$$\Phi(h\nu)=\frac{\int_{E_{T2}}^{h\nu-E_{T1}}\rho_a(\epsilon)d\epsilon}{\int_{0}^{h\nu-E_{T1}}\rho_a(\epsilon)d\epsilon},$$

where $\rho_a(\epsilon)$ is the density of states of the polyatomic first-generation fragment ion.

The probability $\Phi(h\nu)$ is 0 at $h\nu \leqslant E_{T2}$ and eventually becomes 1 as $h\nu\rightarrow\infty$. The rate at which $\Phi(h\nu)$ grows and approaches the full value of 1 depends on the energy gap between E_{T2} and E_{T1}, i.e., on the dissociation energy D_0 of the first-generation ion. The smaller the value of D_0, the sharper the transition of $\Phi(h\nu)$ from 0 to 1. Ultimately, as $E_T - E_{T1}\rightarrow 0$, the two-step process approaches a single-step event, and $\Phi(h\nu)$ becomes a step function, switching abruptly the probability from 0 to 1 at threshold. However, large gaps between E_{T1} and E_{T2} will cause $\Phi(h\nu)$ to grow very slowly and over extended ranges of energy. Assuming that the energy deposition function is not changing substantially in the region of interest, the integral of $\Phi(h\nu)$ defines the inherent shape of the kernel function near threshold

$$Y(h\nu)=A\int_{E_{T2}}^{h\nu}\Phi(\epsilon)d\epsilon.$$

Thus when $E_{T2} = E_{T1}$ and $\Phi(h\nu)$ is a step function, i.e., when there are no fluctuations, $Y(h\nu)$ becomes a linear kernel $Y_1(h\nu)$. In all other cases, $Y(h\nu)$ represents a kernel that is rounded near threshold (*vide infra*), with the amount of curvature related to the rate at which $\Phi(h\nu)$ attains the full value of 1.

The probability function $\Phi(h\nu)$ can be estimated numerically in the region of interest either by exact counting of states or by using some approximate expression for $\rho(E)$, and subsequently fitted with a convenient analytical function. In the case of $CF_2O\rightarrow FCO^+ + F$ followed by $FCO^+\rightarrow CO^+ + F$, the probability $\Phi(h\nu)$, calculated numerically using Haarhoff's expression for density of states,[28] can be very well represented (with a relative error of about 2% or less) by the approximate function

$$\Phi'(h\nu)=1-\exp[-\beta(h\nu-E_{T2})].$$

The parameter β determines the ''spread'' of the fluctuations and is roughly linearly dependent on the selected value for $D_0(\mathrm{F–CO^+})= E_{T2} - E_{T1}$. It also depends on the particular selection of FCO^+ frequencies used as input for the numerical calculation of $\Phi(h\nu)$. However, the exact value of β is inconsequential at this point. The approximate analytical expression $\Phi'(h\nu)$ is very convenient, because the inherent kernel obtained by integrating $\Phi'(h\nu)$ has the form

$$Y_f(h\nu)/A_f=(h\nu-E_{T2})-(1/\beta)\{1-\exp[-\beta(h\nu-E_{T2})]\},$$

where β can now be a fitting parameter and can thus be determined by the shape of the experimental ion yield curve, rather than by a model. Formally, the function $Y_f(h\nu)$ is a superposition of a linear and exponential kernel

$$Y_f(h\nu)/A_f=Y_1(h\nu)/A_1-(1/\beta)Y_e(h\nu)/A_e,$$

with the provision that the original parameter B in the expression for $Y_e(h\nu)$ is substituted with β. However, it is important to note that, as opposed to both $Y_1(h\nu)$ and $Y_e(h\nu)$, which behave linearly near the threshold, the essential behavior of $Y_f(h\nu)$ in the immediate vicinity of the threshold is that of a quadratic function, as can be easily shown by series expansion

$$Y_f(h\nu)/A_f\approx\beta(h\nu-E_{T2})^2/2!-\beta^2(h\nu-E_{T2})^3/3!+\cdots.$$

The solutions of the convolution integral of $Y_f(E)$ with the internal energy distribution function $P(E)$ can be easily obtained from previous solutions for $I_1(h\nu)$ and $I_e(h\nu)$. This leads to the expressions listed below.

(1.1) Pre-threshold region $h\nu < E_{T2}$

$$\begin{aligned}I_f(h\nu)/N_f=(1/a)\{&a(E_{T2}-h\nu)]^{\eta+1}\exp[-a(E_{T2}\\&-h\nu)]+[a(h\nu-E_{T2})+\eta+1]\Gamma[\eta\\&+1,a(E_{T2}-h\nu)]\}-(1/\beta)\{\Gamma[\eta+1,a(E_{T2}\\&-h\nu)]-\exp[-\beta(h\nu-E_{T2})]\Gamma[\eta+1,a(1\\&+\beta/a)(E_{T2}-h\nu)]/(1+\beta/a)^{\eta+1}\},\end{aligned}$$

where $N_f=A_f/\Gamma(\eta+1)$.

(1.2) Post-threshold region $h\nu > E_{T2}$

$$I_f(h\nu)/A_f = (1/a)[a(h\nu - E_{T2}) + \eta + 1] - (1/\beta)\{1 - \exp[-\beta(h\nu - E_{T2})]/(1+\beta/a)^{\eta+1}\}.$$

Both $Y_f(E)$ and $I_1(h\nu)$ are depicted in Fig. 7(c). As with $Y_1(E)$ and $Y_e(E)$, the main effect of the convolution is to shift the curve toward lower energies by $\langle E \rangle$, and to add a rounded tail region. However, since the kernel is already curved in the vicinity of the threshold, it is extremely difficult to obtain E_T by conventional graphical extrapolation.

[1] M. W. Chase, C. A. Davies, J. R. Downey, Jr., D. J. Frurip, R. A. McDonald, and A. N. Syverud, *JANAF Thermochemical Tables*, 3rd ed.; J. Phys. Chem. Ref. Data **14**, Suppl. 1 (1985).
[2] J. A. Montgomery, Jr., H. H. Michels, and J. S. Francisco, Chem. Phys. Lett. **220**, 391 (1994).
[3] L. A. Curtiss, K. Raghavachari, G. S. Trucks, and J. A. Pople, J. Chem. Phys. **94**, 7221 (1991).
[4] G. A. Petersson, T. G. Tensfeldt, and J. A. Montgomery, Jr., J. Chem. Phys. **94**, 6091 (1991).
[5] W. F. Schneider and T. J. Wallington, J. Phys. Chem. **98**, 7448 (1994).
[6] L. A. Curtiss, K. Raghavachari, and J. A. Pople, J. Chem. Phys. **98**, 1293 (1993).
[7] L. Batt and R. Walsh, Int. J. Chem. Kinet. **14**, 933 (1982); **15**, 605 (1983).
[8] W. F. Schneider and T. J. Wallington, J. Phys. Chem. **97**, 12783 (1993).
[9] H. von Wartenberg and G. Riteris, Z. Anorg. Chem. **258**, 356 (1949).
[10] O. Ruff and S.-C. Li, Z. Anorg. Chem. **242**, 272 (1939).
[11] D. R. Stull, E. F. Westrum, Jr., and G. C. Sinke, *The Chemical Thermodynamics of Organic Compounds* (Wiley, New York, 1969), pp. 80–86.
[12] L. V. Gurvich, I. V. Veyts, and C. B. Alcock, *Thermodynamic Properties of Individual Substances*, Vol. 2, 4th ed. (Hemisphere, New York, 1991).
[13] J. C. Amphlett, J. R. Dacey, and G. O. Pritchard, J. Phys. Chem. **7**, 3024 (1971).
[14] H. C. Duus, Ind. Eng. Chem. **47**, 1447 (1955).
[15] *Termicheskiye Konstanty Veshchestv: Spravochnik*, edited by V. P. Glushko (VINITI, Moscow, 1965–1973).
[16] L. A. Curtiss and J. A. Pople (private communication).
[17] J. D. Cox, D.D. Wagman, and V. A. Medvedev, *CODATA Key Values for Thermodynamics* (Hemisphere, New York, 1989).
[18] E. Greenberg and W. N. Hubbard, J. Phys. Chem. **72**, 222 (1968).
[19] T. J. Buckley, R. D. Johson III, R. E. Huie, Z. Zhang, S. C. Kuo, and R. B. Klemm, J. Phys. Chem. **99**, 4879 (1995).
[20] M. W. Farlow, E. H. Man, and C. W. Tullock, Inorg. Syn. **6**, 155 (1960).
[21] P. M. Guyon, W. A Chupka, and J. Berkowitz, J. Chem. Phys. **64**, 1419 (1976).
[22] B. Ruscic and J. Berkowitz, J. Chem. Phys. **98**, 2568 (1993).
[23] C. R. Brundle, M. B. Robin, N. A. Kuebler, and H. Basch, J. Am. Chem. Soc. **94**, 1451 (1972).
[24] R. K. Thomas and H. Thompson, Proc. R. Soc. London Ser. A **327**, 13 (1972).
[25] S. G. Lias, J. E. Bartmess, J. F. Liebman, J. L. Holmes, R. D. Levin, and W. G. Mallard, J. Phys. Chem. Ref. Data **17**, Suppl. 1 (1988).
[26] C. E. Theodosiou, M. Inokuti, and S. T. Manson, At. Data **35**, 473 (1986).
[27] (a) B. Ruscic and J. Berkowitz, J. Phys. Chem. **97**, 11451 (1993); (b) J. Chem. Phys. **100**, 4498 (1994); (c) **101**, 7795 (1994); (d) **101**, 7975 (1994); (e) **101**, 10936 (1994).
[28] P. C. Haarhoff, Mol. Phys. **7**, 101 (1963).
[29] P. D. Mallinson, D. C. McKean, J. H. Holloway, and I. A. Oxton, Spectrochim. Acta A **31**, 143 (1975).
[30] See, for example, G. N. Lewis and M. Randall, *Thermodynamics*, 2nd ed. (McGraw Hill, New York, 1961).
[31] K. P. Huber and G. Herzberg, *Molecular Spectra and Molecular Structure. IV. Constants of Diatomic Molecules* (Van Nostrand, New York, 1979).
[32] (a) W. Forst, *Theory of Unimolecular Reactions* (Academic, New York 1973); (b) Z. Prasil and W. Forst, J. Phys. Chem. **71**, 3166 (1967); (c) M. B. Wallenstein and M. Krauss, J. Chem. Phys. **34**, 929 (1961).
[33] J. M. Dyke, N. Jonathan, A. Morris, and M. J. Winter, J. Chem. Soc. Faraday Trans 2 **77**, 667 (1981).
[34] J. M. Dyke, N. B. H. Jonathan, A. Morris, and M. J. Winter, Mol. Phys. **39**, 629 (1980); J. M. Dyke, J. Chem. Soc. Faraday Trans 2 **83**, 69 (1987).
[35] K. A. G. MacNeil and J. C. J. Thynne, Int. J. Mass Spectrom. Ion Phys. **3**, 35 (1969).
[36] C. Blondel, P. Cacciani, C. Delsart, and R. Trainham, Phys. Rev. A **40**, 3698 (1989).
[37] S. W. Benson, J. Phys. Chem. **98**, 2216 (1994).